Materials Research. 2020; 23(5): e20200105
DOI: https://doi.org/10.1590/1980-5373-MR-2020-0105

Fe-Cr-Si Codeposition on Nb-Si based Alloys via Halide Activated Pack Cementation to Improve Oxidation Resistance

Anderson Weslei da Cruz*[a,b]*, Raphael Felca Glória[b], Rafaela de Oliveira Nogueira[b], Nabil Chaia[c], Gilbert Silva[b], Geovani Rodrigues[b]

[a]*Instituto Federal do Sudeste de Minas Gerais, Campus Juiz de Fora, Rua Bernardo Mascarenhas, 1283, CEP: 36080-001, Fábrica, Juiz de Fora, MG, Brasil.*
[b]*Universidade Federal de Itajubá - UNIFEI, Instituto de Engenharia Mecânica - IEM, Av. BPS, 1303, CEP: 37500-903, Itajubá, MG, Brasil.*
[c]*Universidade de São Paulo - USP/EEL, Departamento de Engenharia de Materiais-DEMAR, Estrada Municipal do Campinho, s/n, Campinho, CEP: 12.602-810, Lorena, SP, Brasil.*

Received: March 17, 2019; Revised: July 09, 2020; Accepted: September 09, 2020

The coating formation by Fe-Cr-Si codeposition was done in a single step via Halide Activated Pack Cementation (HAPC) on Nb-Si alloy with the aim of improving the oxidation resistance. The activator salt and temperature selections for HAPC process were obtained by thermodynamic analysis. The isothermal oxidation test results for the coated alloy at 1200 °C for 62 h showed good oxidation resistance. The mass gain was 17.5 mg/cm^2. Furthermore, no cracks and spallation on the oxide layers were observed for the coated alloy after the oxidation test, being that the oxidative kinetics curve is in accordance with the parabolic rate law. On the other hand, total oxidation was observed for the uncoated alloy after 12 h at 1200 °C in the isothermal oxidation test. The mass gain was 49.27 mg/cm^2 and several cracks and spallation on the oxide layers led to a severe oxidation process.

Keywords: *Nb-Si based alloys, Halide Activated Pack Cementation (HAPC process), Fe-Cr-Si Codeposition, Thermodynamic Analysis, Oxidation Resistance.*

1. Introduction

Refractory alloys of Nb-Si system have high melting points (1934 °C for αNb_5Si_3), low densities (7.2 g/cm^2 for Nb_5Si_3) and good mechanical properties at high-temperature[1-3]. Because of these characteristics, the Nb-Si based alloys have great potential for application in the segments of aeroengines/aerospace being that they can operate between 1200-1450 °C. Furthermore, these alloys are good candidates to substitute Ni-based superalloys currently operating at a maximum temperature of about 1150 °C and a density of about 20% higher than the Nb-Si based alloys[4-8].

Considering the microstructural formation of Nb-Si based alloys, Nb_{ss} (Niobium Solid Solution) and Nb-silicide (Nb_5Si_3 and/or Nb_3Si), the intermetallic phases are responsible for improving of the oxidation and creep resistance[9]. Although silicide phases allow improving the oxidation resistance of the Nb-Si based alloys, their oxidation resistance is not enough when long-term application at ultrahigh-temperature (>1200 °C) are considered[1,8,10]. The development of Nb-Si based alloys, with the addition of certain alloying elements such as Cr, Al, Ti, Sn and Ge improves the oxidation resistance[3,4,11]. On the other hand, in order to establish a protective oxide layer, high contents of these elements are introduced in the alloy which can irreversibly alter its mechanical properties[2,7]. In this way, surface coating is an effective way to improve the oxidation resistance of these alloys while maintaining their mechanical properties.

The surface coatings by HAPC process has been widely applied in different types of materials[11-14]. In this technique, the substrate (alloy to be coated) is introduced into a powder mixture formed by masteralloy (coating elements to be deposited on the surface), activator salt, and inert material (usually Al_2O_3 or SiO_2). In high-temperature conditions, several halide gaseous species are formed due to the reaction between the masteralloy and activator salt. The coating is formed by decomposition of these gaseous species on the substrate surface followed by solid-state diffusion of the coating elements into the substrate. Different types of activating salts can be used in the HAPC process, such as NH_4Cl, NaF, KBr and many others. The selection of an activator type can be done by thermodynamic analysis that allow for the evaluation of the conditions conducive to the coating formation[15-17].

An improvement in the oxidation resistance of Nb-Si based alloys has been performed via HAPC process by deposition and codeposition of elements such as Si, Al, Mo, B, Cr, Ti and Fe[4,7,18-20]. In spite of efforts to develop modified aluminide coating, the silicate-based coatings have greater potential for protection at high-temperatures[5,21,22]. In this case, when modified with Fe and Cr, it is possible to obtain coatings with better oxidation resistance and the coated formed does not affect the strength at temperatures above 1100 °C[23].

*e-mail: anderson.dacruz@ifsudestemg.edu.br

The Fe-Cr-Si codeposition via HAPC process in a single step was successfully performed on Nb-alloys with the formation of complex coatings in multiphase microstructures[18,24]. Oxidative protection is the result of the formation of oxide barriers such as Cr_2O_3 and SiO_2 on the surface, when thermally oxidized in the presence of atmospheric air that prevents oxygen from penetrating the substrate[25].

Although Fe-Cr-Si codeposition has been performed for Nb-based alloys[18,24], the literature lacks a discussion about thermodynamic analysis of the HAPC process. Thus, in the present study, a thermodynamic analysis was performed to select the activator salt type and temperature in the HAPC process that provides the best coating. For this, an alloy of Nb-Si with a high volume fraction of Nb_5Si_3 phase was coated by Fe-Cr-Si codeposition via HAPC process. The evaluation of the protective coating was performed by isothermal oxidation test at 1200 °C.

2. Experimental Procedures

2.1. Thermodynamic analysis

The objective of the thermodynamic analysis is to select the activator salt and temperature in the HAPC process that provides conditions for the codeposition of Fe-Cr-Si on substrate. For this, the thermodynamic analysis was performed using HSC Chemistry 6.0 software based on Gibbs Energy Minimization (GEM) to calculate heterogeneous equilibria occurring during the HAPC process and some activating salts based on chlorides, fluorides, and bromides as NH_4Cl, NaF and KBr, respectively.

The deposition of the gaseous species for the coating formation is directly related to the partial pressures formed during the reaction between the activator and masteralloy. The codeposition is achieved when the partial pressures of different halide gaseous species formed are the highest possible and close to each other[16,26]. High partial pressures indicate high stability of the gaseous species, which can induce important fluxes between the substrate and the gaseous phase and consequently result in the fast kinetic growth of the coating layers[27]. For the thermodynamic analysis in the present study, the composition of the masteralloy was in the ratio 30:20:50 of Fe, Cr and Si, respectively[18].

2.2. Specimen preparation

An Nb-Si alloy with microstructure formed of high volume Nb_5Si_3 phase was obtained by the nominal composition 62.5Nb-37.5Si (at. %). The Nb-Si alloy was produced from high-purity materials, Nb (min. 99.99 wt. %) and Si (min. 99.99 wt. %), by arc-melting with argon atmosphere (min. 99.995%) and using a non-consumable tungsten electrode. The as-cast alloy was heat-treated at 1450 °C for 48 h with argon atmosphere establish equilibrium microstructure. The samples for metallographic observations were cut using a precision blade, embedded in epoxy resin, ground with SiC paper up to #1200 grit, polished with alumina suspension (0.05 μm) and then ultrasonically cleaned in acetone and ethanol and dried with hot air.

2.3. Coating process

The masteralloy was produced with a nominal composition of 30Fe-20Cr-50Si (wt. %) by arc-melting and using high-purity elements Fe (min. 99.99 wt. %), Cr (min. 99.99 wt. %) and Si (min. 99.99 wt. %). Posteriorly, the masteralloy was reduced into a fine powder to optimize its chemical reactivity using agate mortar and pestle. The composition in the pack mixture was 60 wt. % of Fe-Cr-Si masteralloy, 40 wt. % of Al_2O_3 and 15 mg of activator salt, all placed in a 15 cm^3 quartz tube sealed under primary vacuum. The codeposition via HAPC process was carried out in a single step at 1200 °C for 12 h according to thermodynamic analysis.

2.4. Oxidation test

In order to evaluate the protective effects of the coating formation via HAPC process, oxidation tests were performed for the uncoated and coated alloys. The isothermal oxidation tests were carried out under atmospheric air at 1200 °C for 62 h. The mass change of the samples was measured by placing them in an alumina crucible and using NETZSCH thermal analysis (STA449F3) with an accuracy of 1 μg.

2.5. Analyzing methods

The microstructural characterization of the substrate, coating and the oxide formation on surface were performed using Scanning Electron Microscopy via Back-Scattered Electron images (SEM/BSE) and Secondary Electron images (SEM/SE) through ZEISS-EVO MA15 equipment. The phases formed in the Nb_5Si_3 alloy before and after heat treatment and the oxide formation on surface were identified by X-Ray Diffraction (XRD) through X'Pert Pro (Panalytical) diffractometer, using Cu-Kα radiation, an angular interval 2θ from 20 to 80, an angular step of 0.05 and 1.0 s counting time. Energy Dispersive X-Ray Analysis (EDXA) was used to evaluate the composition of the coating and oxide formation.

3. Results and Discussion

3.1. Thermodynamic analysis

Figure 1 shows the formation of different activators considering one mol of Cl_2, F_2 and Br_2, from 0 to 1500 °C. It is observed that the thermal decomposition (Gibbs free energy more positive) of chlorides occurs more easily when compared to the decomposition of fluorides and bromides, noting too the wide difference between them. Above 200 °C NH_4Cl activator is more unstable than $CrCl_3$ activator and, as temperature increases, this instability becomes more evident, justifying the previous choice of NH_4Cl as the HAPC process activator because of its ability to decompose more easily and generate the species required for the coating formation reaction.

Figure 2 shows the partial pressure profile of different halide gaseous species formed in the reaction between activating salt with the Fe-Cr-Si masteralloy. The use of NH_4Cl as activator provides a gaseous phase containing mainly the species of $FeCl_2$, $CrCl_2$, $CrCl_3$, $SiCl_2$, $SiCl_3$ and $SiCl_4$, these gaseous species can be considered as vectors of Fe, Cr and Si from the gas phase to the substrate. It is important to note that the higher the partial pressure of

gaseous species the greater the activity of these species in the coating formation. Furthermore, it is observed that from 1200 °C most of these species have a steeper decline in their partial pressures, so this would be the maximum temperature for the HAPC process and maximum activity in its process.

The halide gaseous species with partial pressures less than 10^{-5} bar has no significant influence on the deposition process and those with values below 10^{-8} bar were excluded from the plot because the deposition is made difficult by the low partial pressure. Another important detail is the proximity of the partial pressure profiles of the gaseous species, being that the codeposition of Fe, Cr, and Si can occur at the same time.

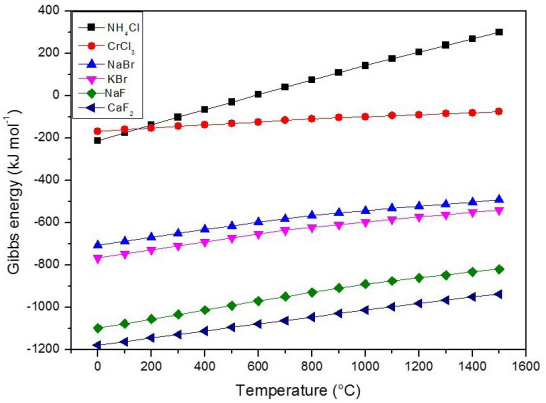

Figure 1. Gibbs free energy of formation for different activating salts as a function of temperature.

In the case of using any other activator for the deposition of gaseous species, the gas phase generated may be very different, as observed in Figure 2 for activating salts such as NaF and KBr. For the HAPC process activated by NaF, at temperature range of 1000 to 1500 °C, there are only the formations of the silicon gaseous species (SiF_4, SiF_3, SiF_2 and SiF), therefore there would only be Si deposition on the substrate. For the HAPC process activated by KBr, the partial pressures of gaseous species are very low (below 10^{-6} bar) and there are only the formations of Fe and Si halide gaseous species at 1200 °C. Thus, Cr deposition would not occur and there would probably be only a minimum Fe-Si codeposition.

Therefore, considering the analysis of the Gibbs free energy of formation in Figure 1 and the studies of the halide gas phases in Figure 2, the codeposition of Fe, Cr, and Si would have better conditions in a process activated by NH_4Cl at 1200 °C.

3.2. Uncoated alloy characterization

Figure 3 shows microstructural characterization of the uncoated alloy in the as-cast condition and after being heat treated at 1450 °C for 48 h. In Figure 3A it can be seen that in the as-cast condition, the alloy is constituted by βNb_5Si_3 phase, a situation of non-thermodynamic equilibrium. After the heat treatment, the alloy is constituted by αNb_5Si_3 and

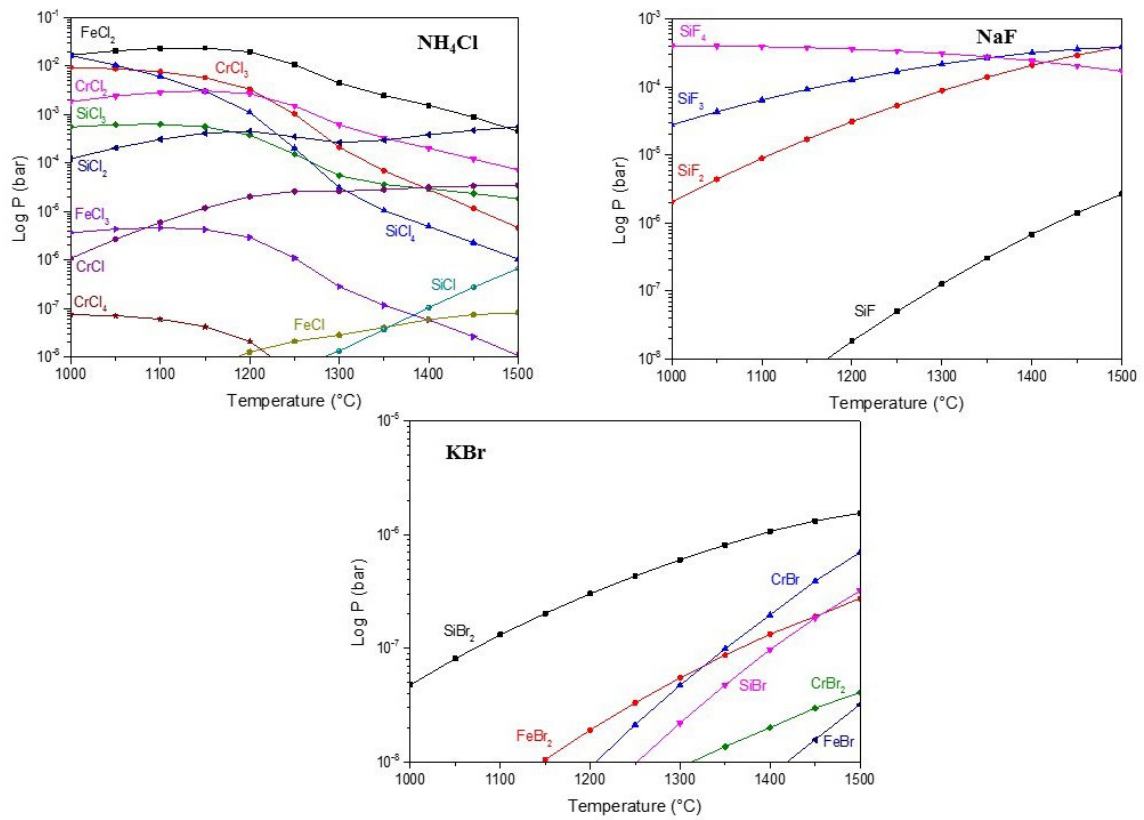

Figure 2. Equilibrium partial pressure of Fe, Cr and Si halide gaseous species involving the reaction of Fe-Cr-Si masteralloy with different activating salts.

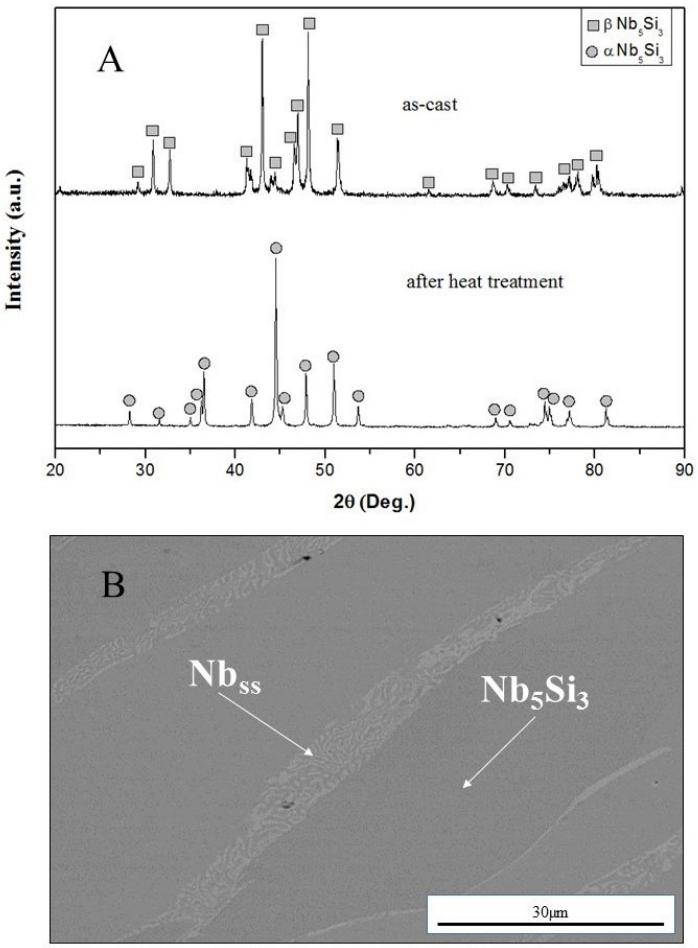

Figure 3. A X-Ray Diffraction before and after the heat treatment of the Nb-Si alloy and **B** SEM/BSE image of the microstructure of the Nb-Si alloy after the heat treatment at 1450 °C/48 h.

Nb_{ss} phases, indicating thermodynamic equilibrium as showed in Figure 3B by SEM/BSE image. In this case, the Nb_{ss} phase does not appear in the diffractogram (Figure 3A) due to the fact that the most intense peak of Nb_{ss} phase coincides with the peak of the αNb_5Si_3 phase at 2θ=38.507°. Taking into account that the alloy with nominal composition 62.5Nb-37.5Si (at. %) is in the single phase field (Nb_5Si_3), the presence of the Nb_{ss} phase is associated with a possible loss of Si during the arc melting stage.

3.3. Fe-Cr-Si codeposition on Nb-Si alloy via HAPC process

Figure 4A shows the cross-section by SEM/BSE image after Fe-Cr-Si codeposition on Nb-Si alloy (substrate) via HAPC process. For the conditions indicated by the thermodynamic analysis, a successful coating was obtained for practical application. The coating formation showed a good chemical homogeneity, uniform thickness and a complete covering on the surface of substrate. In addition, the results showed a coating formed by multiphase microstructure consisting of four layers to be referred to as: outer layer, intermediate layer, inner layer and diffusion zone. The average thickness of the diffusion zone, inner and intermediate layer was 26.1 μm and the outer layer was 10.5 μm, resulting in a coating thickness of 36.6 μm. Moreover, the layers of the diffusion zone, inner and intermediate showed a uniform and homogeneous formation. The absence of pores and voids near the interface implies good adherence between the coating and substrate[28]. On the other hand, it is observed that the outer layer showed the formation of pores and voids, which do not decrease the oxidation resistance of the coating, but only of the outer layer.

Figure 4B show the concentrations profiles of Fe, Cr, Si e Nb elements along the coating thickness. The exact position of the measurement points can be seen in Figure 4A. It can be observed that the chromium concentration starts at 50.27 at. % in the outer layer (point 1) and progressively decreases in the adjacent coating layers (points 2-7). The silicon concentration starts at 36 at. % in the outer layer (point 1) and continuously increased to about 42 at. % in the intermediate layer (point 2), then remained constant along the intermediate layer and in part of the inner layer (points 3-4, respectively). At points 5-7 the silicon concentration is close to the alloy composition, about 37.5 at. %. The iron concentration starts at 26 at. % in the outer layer (point 1) and declines to 18 at. % in the intermediate layer (points 2-3).

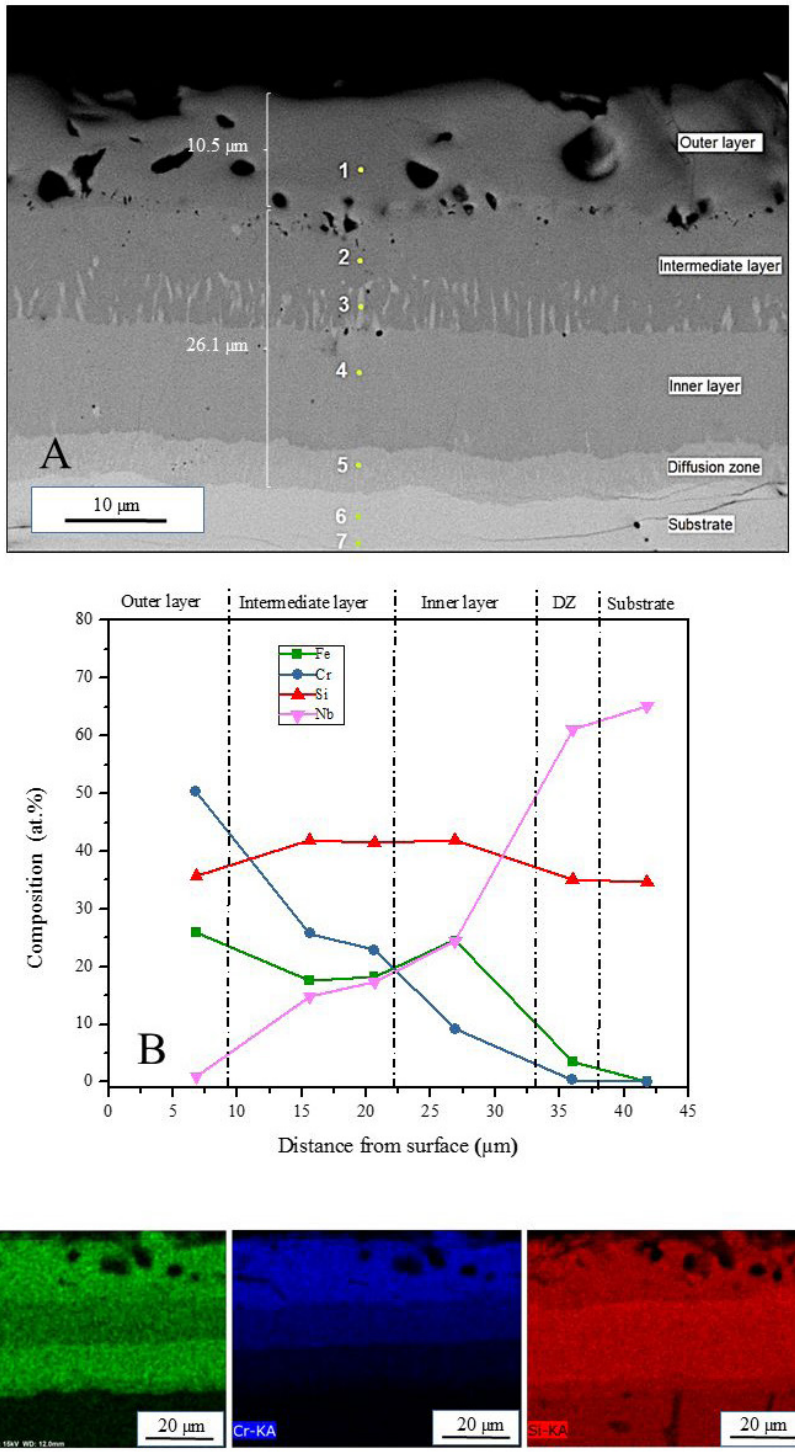

Figure 4. A Cross section by SEM/BSE image of the coating formed at 1200 °C for 12 h in a pack mixture of 60 wt. % (Fe-Cr-Si masteralloy)-40 wt.% Al_2O_3-15 mg NH_4Cl, **B** EDXA concentration profiles of coating elements and **C** EDXA mapping of the coating elements.

Then iron concentration increased in the inner layer, to about 24.5 at. % at point 4 and finally decrease to minimum levels in the points 5 to 7. The presence of chromium and silicon content along the coating thickness improves the oxidation resistance of the alloy through oxide formation on the surface after oxidation at high temperatures. This variation in the concentration profiles can be also visualized in Figure 4C, which shows the mapping of the coating layer by EDXA.

EDS analysis showed that the coating layer is formed by phases with compositions close to $NbFe_5Cr_5Si_8$ (outer

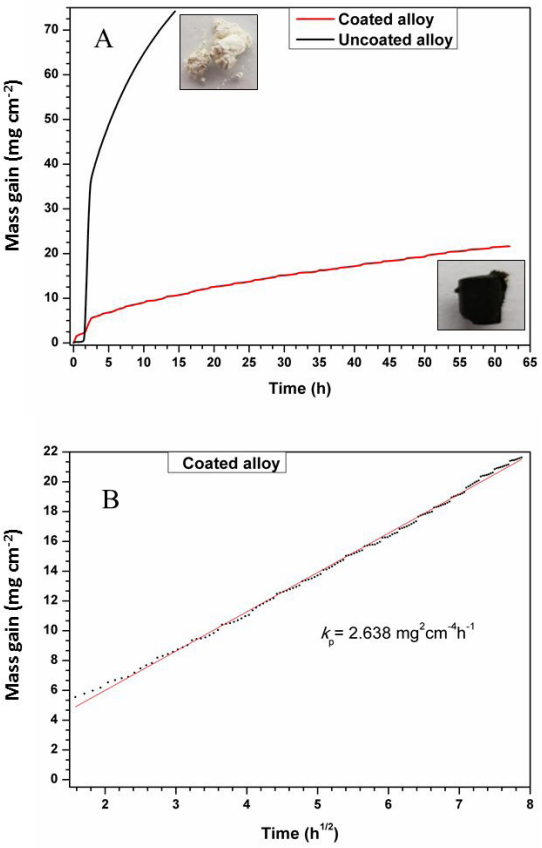

Figure 5. A Oxidation kinetics at 1200 °C for 62 h in the air for uncoated and coated alloys and **B** linear plot for the coated alloy.

layer), $Nb_2Fe_2Cr_2Si_5$ (middle layer), $Nb_3Fe_3CrSi_6$ (inner layer), NbFeSi and Nb_2FeSi_2 (diffusion) zone, according to the Vilasi et al.[24].

3.4. Isothermal oxidation tests

Figure 5A show the results for the oxidation tests at 1200 °C for 62 h involving the uncoated and coated alloys. For the uncoated alloy, the sample undergoes high oxidation with a mass gain of 49.27 mg/cm^2 after 12 h at 1200 °C in air being completely oxidized. In contrast, the coated alloy showed good oxidation resistance with a mass gain of 17.5 mg/cm^2 after 62 h at 1200 °C. The total oxidation for the uncoated alloy suggests the formation of cracks and spallation on the oxide layers during exposure at high temperature. Hence, the oxygen penetrates into the substrate leading to rapid continuous oxidation reaction at the metal/oxide interface. In opposition, the coated alloy did not undergo severe oxidation since this later maintained its integrity after the oxidation test, as illustrated in Figure 5A. For the coated alloy, the oxidation kinetic curve followed a parabolic-like law during the isothermal oxidation test. The parabolic rate constant calculated from plot of mass change versus the square root of time for the coated alloy is approximately 2.64 mg^2/cm^4·h, as shown in Figure 5B.

Figure 6A shows the surface of the coated sample after the oxidation test by SEM/SE image. Again, no cracks and spallation on the surface oxide layers were observed. Figure 6B shows the presence of elements of Fe, Cr, Si, and Nb on the oxidized surface by EDXA mapping. It is observed that the chromium (blue color) is the major element followed by minor proportions of silicon (red color) and iron (green color)/niobium (yellow color), respectively.

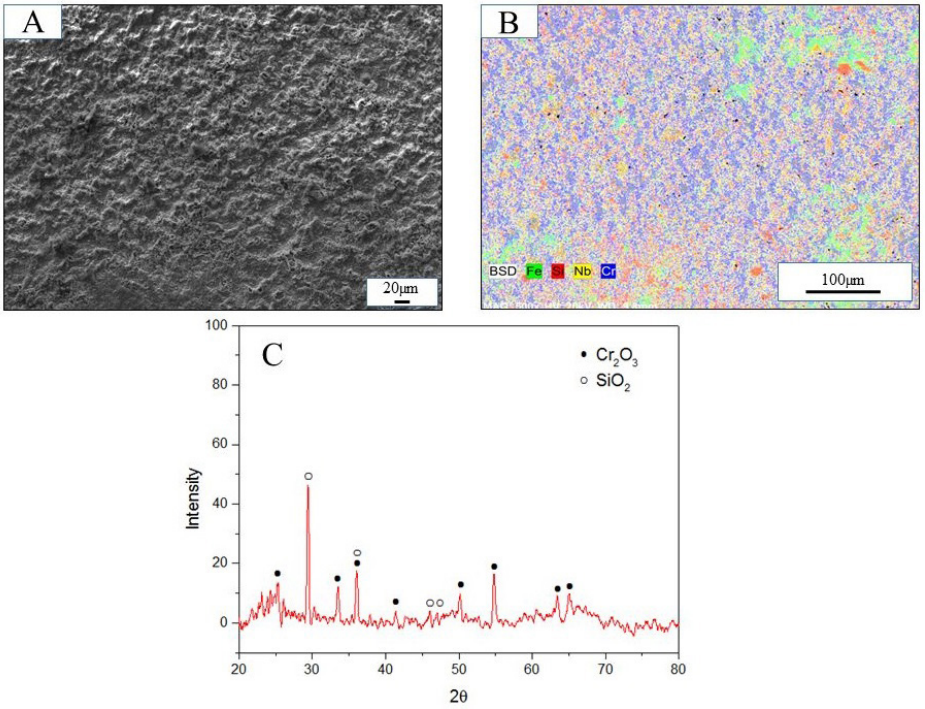

Figure 6. Images on the surface oxide layer after the oxidation test for the coated alloy being: **A** SEM/SE image, **B** EDXA mapping and **C** X-Ray Diffraction.

Table 1. Results of several oxidation test reports for Nb-Si based alloys being considered uncoated alloys with alloying elements and coated alloys via HAPC process.

Alloys (at. %)	Masteralloy	Deposition Condition (°C/h) and Salt Activator	Coating Thickness (μm)	Oxidation Test (°C/h)	Change Mass (mg cm^{-2})	K_p (mg^2 $cm^{-4}h^{-1}$)
Present work						
Nb_{ss}/Nb_5Si_3 (62.5Nb-37.5Si)	-	-	-	1200/12	74	-
Nb_{ss}/Nb_5Si_3 (62.5Nb-37.5Si)	Fe-Cr-Si	1200/12 NH_4Cl	36.6	1200/62	21	2.69
Coated alloy via HAPC process						
Nb_{ss} [19]	Si	1100/7 MgF_2	110	1200/50	6.67	-
Nb_{ss} [18]	Nb-Fe-Cr-Si	1200/24 $CrCl_3$	38	1100/90	2.1	-
Nb_{ss} (Nb-8.9Hf-1.2Zr)[20]	Si	1300/8 NaF	100	1250/50	6.5	0.79
$Nb/NbCr_2$ (Nb-35Cr)[29]	Si-Y	1250/8 NaF	200	1250/50	13.1	5.1
Nb_{ss}/Nb_5Si_3 (Nb-16Si-22Ti-17Cr-2Al-2Hf)[1]	Si-B-Ti	1300/10 NaF	162	1250/100	2.39	0.22
Nb_{ss}/Nb_5Si_3 (Nb-15Si-24Ti-4Cr-2Al-2Hf)[4]	Mo-Si-B	1000/25 NaF	50	1300/24	-0.55	-
Nb_{ss}/Nb_5Si_3 (Nb-16Si-25Ti-2Cr-2Al-8Hf)[8]	Nb-Ti-Fe-Cr-Si	1200/24 $CrCl_3$	50	1200/50	1.1	0.019
Nb_{ss}/Nb_5Si_3 (Nb-16Si-22Ti-17Cr-2Al-8Hf)[11]	Si-Ge	1300/10 NaF	176	1250/100	16.3	-
Nb_{ss}/Nb_5Si_3 (Nb-16Si-22Ti-17Cr-2Al-8Hf)[11]	Si	-	-	1250/100	5.42	-
Nb_{ss}/Nb_5Si_3 (Nb-16Si-20Ti-6Cr-4Al-5Hf-2B-0.06Y)[30]	Si-Al-Y	1050/10 NaF	49	1250/100	50	62.6
Nb_{ss}/Nb_5Si_3 (Nb-14.3Si-39.4Ti-4.9Cr-3Al-2.8Hf)[31]	Si-B	1150/8 NaF	60	1250/100	2.8	5.70×10^{-2}
Uncoated alloy						
Nb_{ss}/Nb_5Si_3 (Nb-16Si-22Ti-17Cr-2Al-2Hf)[1]	-	-	-	1250/100	190.08	-
Nb_{ss}/Nb_5Si_3 (Nb-15Si-24Ti-4Cr-2Al-2Hf)[4]	-	-	-	1300/24	87.6	-
Nb_{ss}/Nb_5Si_3 (Nb-18Si-24Ti-2Cr-2Al-8Hf)[10]	-	-	-	1250/50	198.91	1220
Nb_{ss}/Nb_5Si_3 (Nb-18Si-24Ti-2Cr-2Al-8Hf)[10]	-	-	-	1250/50	96.48	220
$Nbss/Nb5Si_3$ (Nb-16Si-24Ti-10Cr-2Al-2Hf)[32]	-	-	-	1200/100	134	-
$Nbss/Nb5Si_3$ (Nb-16Si-24Ti-17Cr-6Al-2Hf)[32]	-	-	-	1200/100	18.9	1.897

In this case, the presence of the chromium and silicon elements constitute the oxides formed on the oxidized surface, shown in Figure 6C by X-Ray Diffraction. Thus, the formation of oxides of chromium and silicon were responsible for the increasing oxidation resistance of the coated alloy.

Table 1 lists several studies related to oxidation tests involving Nb-Si based alloys. The Fe-Cr-Si coating applied to Nb_{ss}/Nb_5Si_3 alloy in this work showed significant improvements in oxidation resistance compared to uncoated alloys from other studies containing various elements in its compositions, such as Al and Cr, which provide this resistance, except for an alloy containing a high concentration of these elements presented by the work of Su et al.[32]. On the other hand, other types of coatings presented in Table 1 have shown to be better in oxidation tests when compared to the coated alloy of this study, showing values below 2.638 $mg^2/cm^4.h$, with the exception of two alloys coated with Si-Al-Y[30] and Si-Y[29], with values of 62.6 and 5.1 $mg^2/cm^4.h$, respectively.

Moreover, the evaluation of the lifetime coatings and their behavior for the oxidation tests involve qualitative parameters of the coating (adhesion, cracks, voids) as well as quantitative aspects of composition of the coatings and phases formed. Thus, in relation to the present study, the presence of cracks in the substrate that extends to the coating might have had a negative effect in reducing its oxidation resistance.

4. Conclusions

Fe-Cr-Si Codeposition via HAPC process in a single step and activated by NH_4Cl was performed for the formation of a coating on Nb-Si alloy to improve oxidation resistance. The thermodynamic analysis was successfully used for selection of codeposition parameters; namely, the temperature and the activator nature. The conclusions that were drawn from the present study can be summarized as follows:

- From the thermodynamic analysis performed with different activating salts (NH_4Cl, NaF and KBr), the calculations suggested that the NH_4Cl activator was better for the codeposition of Fe, Cr and Si elements at 1200 °C. In this case, the formation of gaseous species based on Cr, Si and Fe with high partial pressure and close to each other were crucial to promote the coating growth;
- A multiphase microstructure formed of four layers was obtained on the coated surface of the Nb-Si alloy. The presence of the coating elements (Fe-Cr-Si) was verified in the coating formed by EDXA results. Thus, the chromium and silicon content along the thickness of the coating improved the oxidation resistance of the alloy through the formation of protective oxides during exposure at high temperatures. The total thickness of the coating was approximately 37 μm. The inner layers of the coating, with a thickness near 26 μm, exhibited a uniform and homogeneous aspect with the absence of pores and voids which is desired for an improved oxidation resistance. The outer layer exhibited the formation of pores and voids with a thickness near 10 μm which may in part explain the relatively lower oxidation resistance compared to other coating from the literature;
- The oxidation tests showed an improvement in the oxidation resistance for the coated alloy as opposed to total oxidation of the uncoated alloy. The coated alloy had a mass gain of 17.5 mg/cm^2 after 62 h at 1200 °C, almost three times smaller than the uncoated alloy, which had a mass gain of 49.27 mg/cm^2 after 12 h at 1200 °C. The oxidation kinetic curve for the coated alloy followed a parabolic law with a rate constant determined to be 2.638 $mg^2/cm^4.h$, approximately. The formation of SiO_2 and Cr_2O_3 oxide scales on the surface of the coating contributed to enhancing the oxidation resistance of the alloy.

5. Acknowledgements

The authors gratefully acknowledge the financial support from CAPES, CNPq and FAPEMIG. The technical support from University of São Paulo-USP/EEL is gratefully acknowledged.

6. References

1. Shao W, Wang W, Zhou C. Deposition of a B-modified silicide coating for Nb-Si based alloy oxidation protection. Corros Sci. 2016;111:786-92.
2. Shiyu QU, Yafang H, Liguo S. Microstructures and properties of refractory niobium-silicide-based composites. Mater Sci Forum. 2005;475-479:737-40.
3. Utton CA, Papadimitriou I, Kinoshita H, Tsakiropoulos P. Experimental and thermodynamic assessment of the Ge-Nb-Si ternary phase diagram. J Alloys Compd. 2017;717:303-16.
4. Su L, Lu-Steffes O, Zhang H, Perepezko JH. An ultra-high temperature Mo-Si-B based coating for oxidation protection of Nb_{ss}/Nb_5Si_3 composites. Appl Surf Sci. 2015;337:37-44.
5. Vilasi M, Francois M, Brequel H, Podor R, Venturini G, Steinmetz J. Phase equilibria in the Nb-Fe-Cr-Si system. J Alloys Compd. 1998;269:187-92.
6. Braun R, Schulz U, Portebois L, Mathieu S, Vilasi M. Environmental protection of Nb/Nb_5Si_3-based alloys by E/TBC systems. Intermetallics. 2018;93:169-79.
7. Zhang S, Guo X. Alloying effects on the microstructure and properties of Nb-Si based ultrahigh temperature alloys. Intermetallics. 2016;70:33-44.
8. Knittel S, Mathieu S, Portebois L, Drawin S, Vilasi M. Development of silicide coating to ensure the protection of Nb and silicide composites against high temperature oxidation. Surf Coat Tech. 2013;235:401-6.
9. Kong B, Jia L, Zhang H, Sha J, Shi S, Guan K. Microstructure, mechanical properties and fracture behavior of Nb with minor Si addition. Int J Refract Met Hard Mater. 2016;58:84-91.
10. Guo Y, Jia L, Zhang F, Liu J, Zhang H. Improvement in the oxidation resistance of Nb-Si based alloy by selective laser melting. Corros Sci. 2017;127:260-9.
11. Wang W, Yuan B, Zhou C. Formation and oxidation resistance of germanium modified silicide coating on Nb based in situ composites. Corros Sci. 2014;80:164-8.
12. Lu XJ, Xiang ZD. Formation of chromium nitride coating on carbon steels by pack cementation process. Surf Coat Tech. 2017;309:994-1000.
13. Tang Z, Thom AJ, Kramer MJ, Akinc M. Characterization and oxidation behavior of silicide coating on multiphase Mo-Si-B alloy. Intermetallics. 2008;16:1125-33.

14. Bianco R, Rapp A. Pack cementation aluminide coating on superalloys: codeposition of Cr and reactive elements. The Electrochemical Society. 1993;140:1181-90.
15. Bianco R, Harper MA, Rapp RA. Codepostion elements by Halide Activated Pack Cementation. J Miner Met Mater Soc. 1991;48:20-5.
16. Kung S-C, Rapp RA. Analyses of the gaseous species in Halide-Activated Cementation coating packs. Oxid Met. 1989;32:89-109.
17. Geib FD, Rapp RA. Simultaneous chromizing-aluminizing coating of low-alloy steels by a halide-activated pack cementation process. Oxid Met. 1993;40:213-28.
18. Vilasi M, Francois M, Podor R, Steinmetz J. New silicide for new niobium protective coating. J Alloys Compd. 1998;264:244-51.
19. Choi YJ, Yoon JK, Kim GH, Yoon WY, Doh JM. High temperature isothermal oxidation behavior of $NbSi_2$ coating at 1000-1450°C. Corros Sci. 2017;129:102-14.
20. Ge Y, Wang Y, Chen J, Zou Y, Guo L, Ouyang J, et al. An Nb_2O_5-SiO_2-Al_2O_3/$NbSi_2$/Nb_5Si_3 multilayer coating on Nb-Hf alloy to improve oxidation resistance. J Alloys Compd. 2018;745:271-81.
21. Majumdar S, Arya A, Sharma IG, Suri AK, Banerjee S. Deposition of aluminide and silicide based protective coating on niobium. Appl Surf Sci. 2010;257:635-40.
22. Tian X, Guo X. Structure of Al-modified silicide coating on an Nb-based ultrahigh temperature alloy prepared by pack cementation techniques. Surf Coat Tech. 2009;203:1161-6.
23. Kumawat MK, Alam MZ, Kumar A, Gopinath K, Saha S, Singh V, et al. Tensile behavior of a slurry Fe-Cr-Si coated Nb-alloy evaluated by Gleeble testing. Surf Coat Tech. 2018;349:695-706.
24. Vilasi M, Bréquel H, Podor R, Steinmetz J. Silicide coating for niobium alloys. In N.B. Dahotre, J. M. Hampikian, editors. Elevated temperature coatings: science and technology II. Pittsburgh: The Minerals, Metals and Materials Society; 1996. p. 233-242.
25. Chen C, Zhou C, Gong S, Li S, Zhang Y, Xu H. Deposition of Cr-modified silicide coatings on Nb-Si system intermetallics. Intermetallics. 2007;15:805-9.
26. Schmidt D, Galetz M, Schütze M. Deposition of manganese and cobalt on ferritic martensitic steels via pack cementation. Oxid Met. 2013;79:589-99.
27. Lu XJ, Xiang ZD. Formation of chromium nitride coating on carbon steels by pack cementation process. Surf Coat Tech. 2017;309:994-1000.
28. Chaliampalias D, Stergioudis G, Skolianos S, Vourlias G. The effect of the deposition temperature and activator concentration on the structure of NiCrBSi coating deposited on low carbon steels by pack cementation process. Mater Lett. 2008;62:4091-3.
29. Qiao Y, Li M, Guo X. Development of silicide coatings over Nb-$NbCr_2$ alloy their oxidation behavior at 1250°C. Surf Coat Tech. 2014;258:921-30.
30. Zhang P, Guo X. A comparative study of two kinds of Y and Al modified silicide coating on an Nb-Ti-Si based alloy prepared by pack cementation technique. Corros Sci. 2011;53:4291-9.
31. Qiao Y, Shen Z, Guo X. Co-depostion of Si and B to form oxidation-resistant coatings on an Nb-Ti-Si based ultrahigh temperature alloy by pack cementation technique. Corros Sci. 2015;93:126-37.
32. Su L, Jia L, Jiang K, Zhang H. The oxidation behavior of high Cr and Al containing Nb-Si-Ti-Hf-Al-Cr alloys at 1200°C and 1250°C. Int J Refract Met Hard Mater. 2017;69:131-7.